NANO MICRO small

Supporting Information

for *Small,* DOI: 10.1002/smll.202107832

Plasmonic LAMP: Improving the Detection Specificity and Sensitivity for SARS-CoV-2 by Plasmonic Sensing of Isothermally Amplified Nucleic Acids

Haihang Ye, Chance Nowak, Yaning Liu, Yi Li, Tingting Zhang, Leonidas Bleris, and Zhenpeng Qin**

Supporting Information for

Plasmonic LAMP: Improving the Detection Specificity and Sensitivity for SARS-CoV-2 by Plasmonic Sensing of Isothermally Amplified Nucleic Acids

Haihang Ye,[†] Chance Nowak,[‡,|] Yaning Liu,[†] Yi Li,[‡,§] Tingting Zhang,[†] Leonidas Bleris,[*,‡,|,§] and Zhenpeng Qin[*,†,⁑,‖,§]

[†]*Department of Mechanical Engineering, The University of Texas at Dallas, Richardson, Texas 75080, United States*

[‡]*Center of Systems Biology, The University of Texas at Dallas, Richardson, Texas 75080, United States*

[⁑]*Center for Advanced Pain Studies, The University of Texas at Dallas, Richardson, Texas 75080, United States*

[‖]*Department of Surgery, The University of Texas Southwestern Medical Center, Dallas, Texas 75390, United States*

[|]*Department of Biological Sciences, The University of Texas at Dallas, Richardson, Texas 75080, United States*

[§]*Department of Bioengineering, The University of Texas at Dallas, Richardson, Texas 75080, United States*

[*]*Corresponding Author: E-mail: Bleris@utdallas.edu; Zhenpeng.Qin@utdallas.edu*

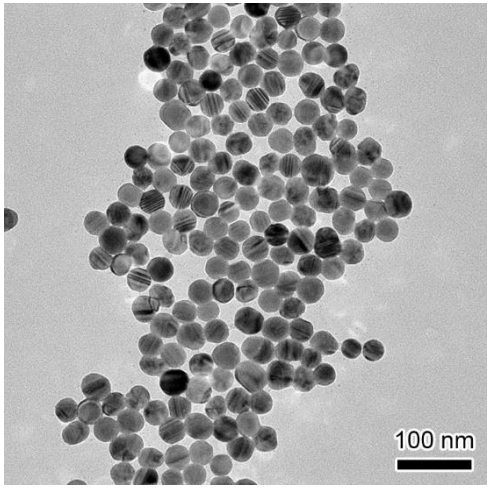

Figure S1. Transmission electron microscopy (TEM) image of AgNPs as templates.

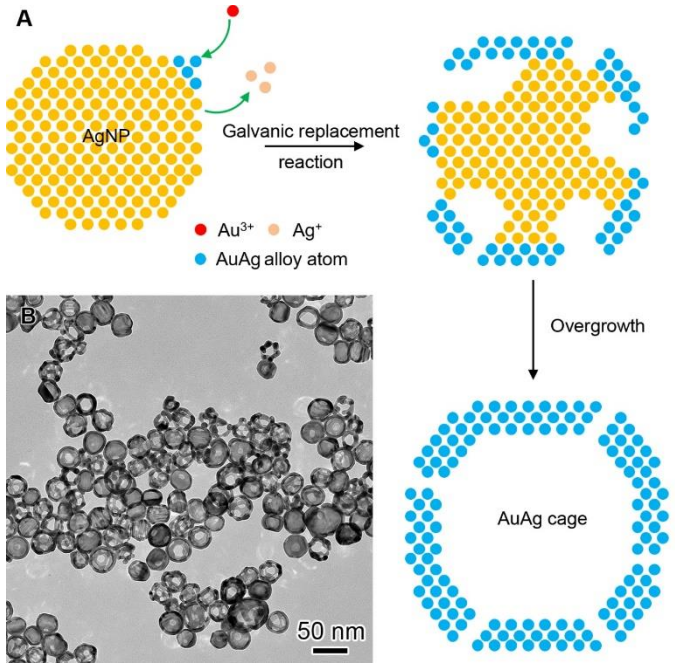

Figure S2. **The preparation of Au-Ag nanocages.** (A) Schematic illustration of the cage growth. (B) TEM image of Au-Ag cages obtained at 0 mM Na_3CA with 3.3 mL $HAuCl_4$ injection.

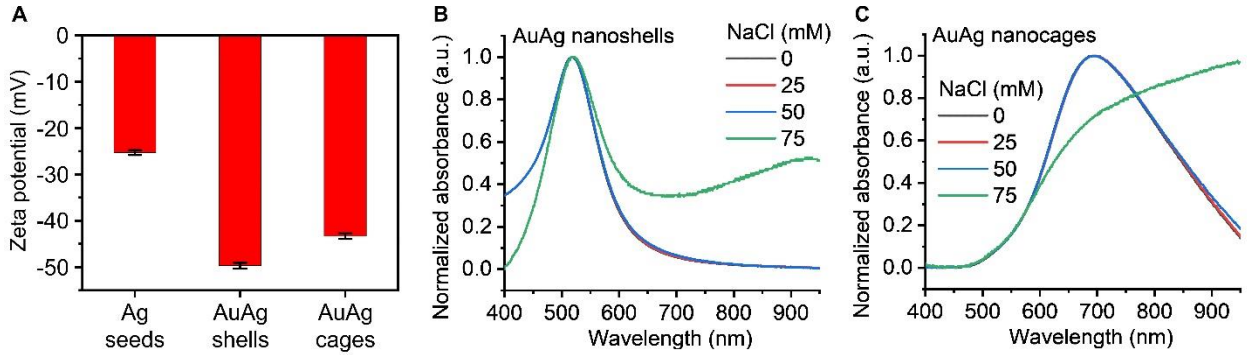

Figure S3. **Colloidal stability test of Ag seeds, AuAg nanoshells (NSs), and AuAg nanocages (NCs).** (A) Zeta potential tests for NPs of different shapes without centrifuge and washing steps. (B, C) Absorption spectra of AuAgNSs (B) and AuAgNCs (C) against sodium chloride (NaCl) solution with varied concentrations. The spectra of both particle suspensions change when mixing with 75 mM NaCl solution, suggesting particle agglomeration. Note the AuAgNSs were obtained in the presence of 2 mM Na_3CA, while the AuAgNCs were obtained in the absence of Na_3CA.

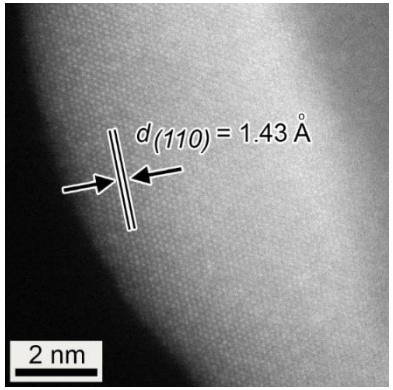

Figure S4. **Atomic-resolution high-angle annular dark-field scanning TEM**. The lattice spacing was measured to be 1.43 Å, corresponding to the (110) plane of Au and Ag alloyed structure.

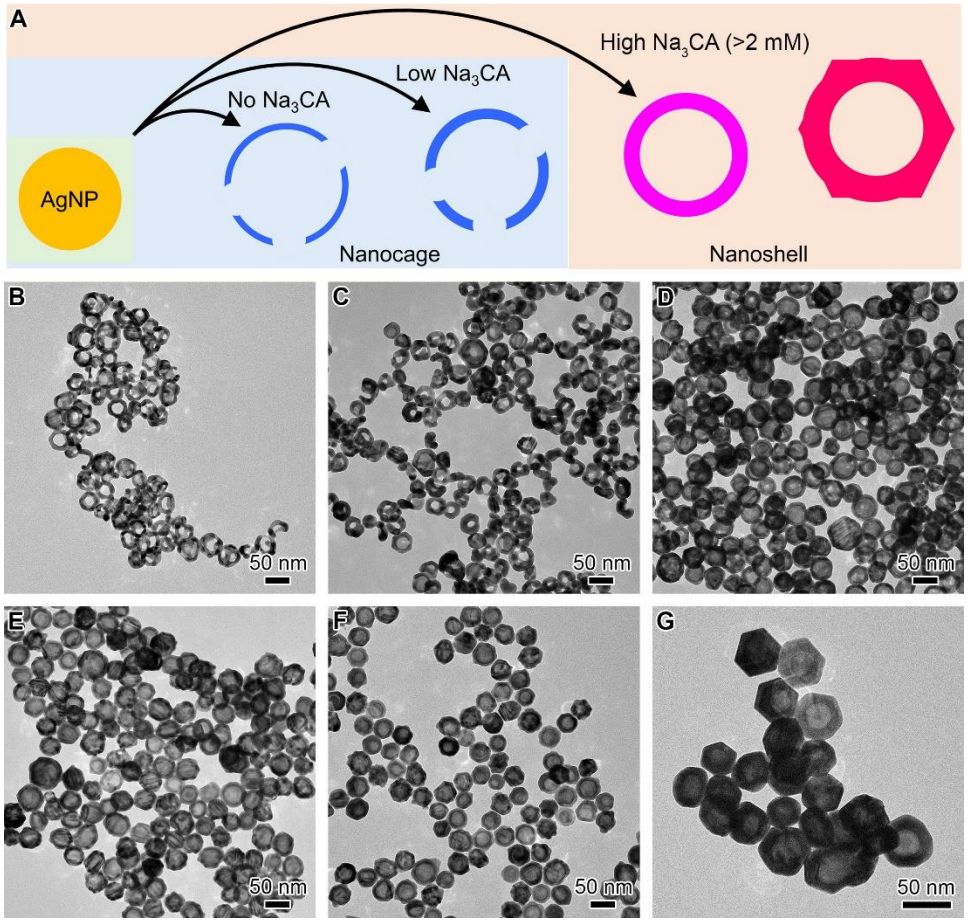

Figure S5. **Morphological characterization of hollow Au-Ag nanostructures obtained at varied concentration of Na_3CA.** (A) Schematic illustration of the growth pathways. (B-G) TEM images of the products obtained in the presence of 0 mM (B), 0.5 mM (C), 1 mM (D), 5 mM (E), 10 mM (F), and 20 mM (G) Na_3CA. In (B), 6 mL of $HAuCl_4$ was injected, while 10 mL $HAuCl_4$ was added for the rest cases.

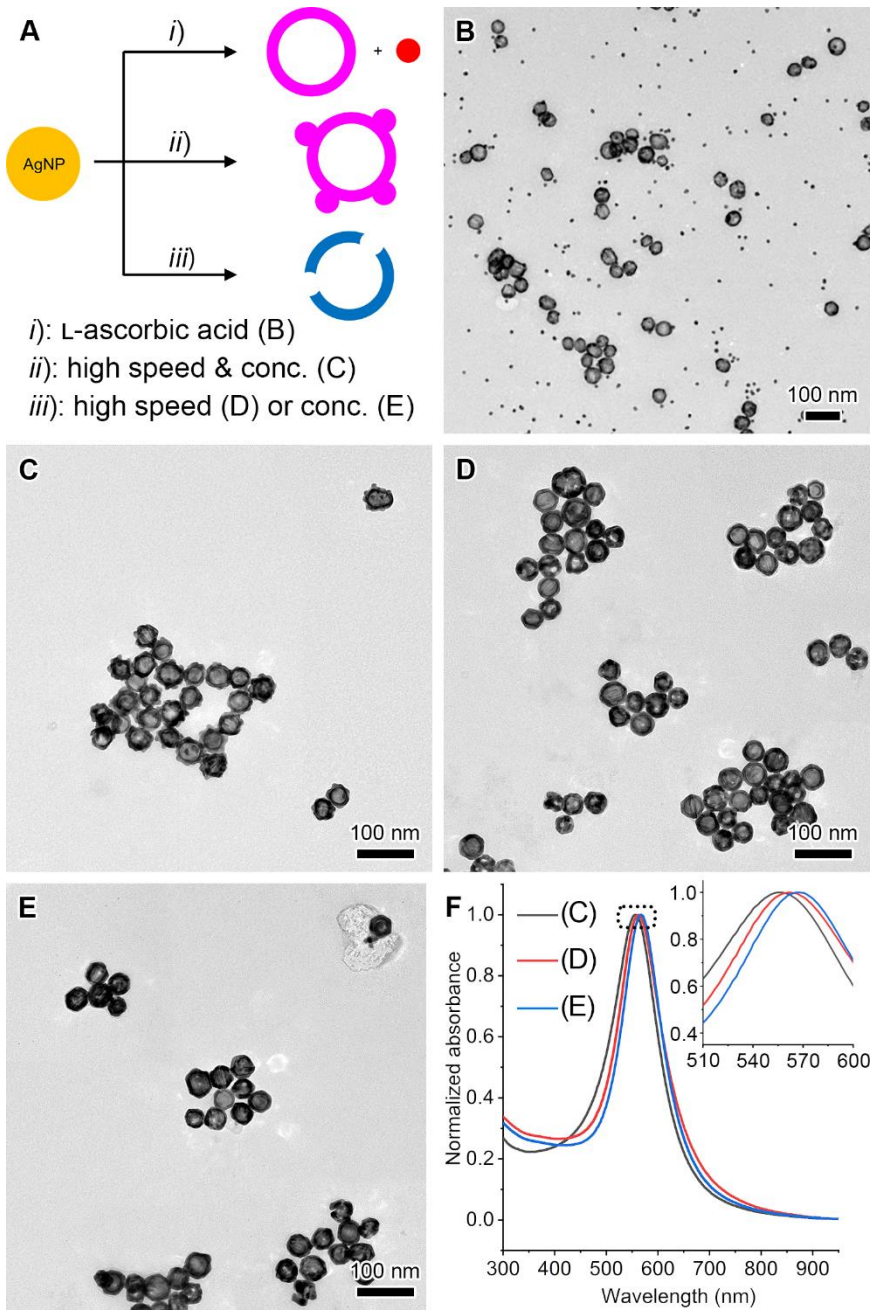
A
i)
ii)
iii)
AgNP
i): L-ascorbic acid (B)
ii): high speed & conc. (C)
iii): high speed (D) or conc. (E)
B
100 nm
C
100 nm
D
100 nm
E
100 nm
F
(C)
(D)
(E)
Normalized absorbance
Wavelength (nm)
1.0
0.8
0.6
0.4
0.2
0.0
300
400
500
600
700
800
900
510
540
570
600

Figure S6. **Morphological and optical characterizations of hollow Au-Ag nanoshells obtained at varied conditions.** (A) Schematic illustration of the different growth conditions: *i*) replacing Na_3CA with 2 mM $_L$-ascorbic acid; *ii*) increase both the inject speed (30 mL/h) and concentration of $HAuCl_4$ (0.04%, w/v); and *iii*) increase either the inject speed to or concentration of $HAuCl_4$. (B-E) TEM images of the correponding products obtained for cases of (*i-iii*), respectively. (F) Normalized extinction spectra showing the corresponding LSPR peaks of the products in (C-E). Inset shows a zoom-in view of the highlighted spectra region (dashed box).

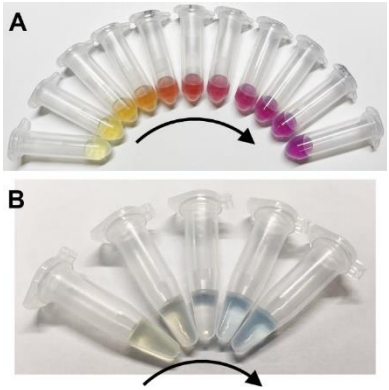

Figure S7. Photographs taken from the aliquots during the synthesis of Au-Ag nanoshells (A) and nanocages (B) in the presence and absence of Na_3CA, respectively. The arrows mark the color change when an increasing amount (per mL) of $HAuCl_4$ was injected.

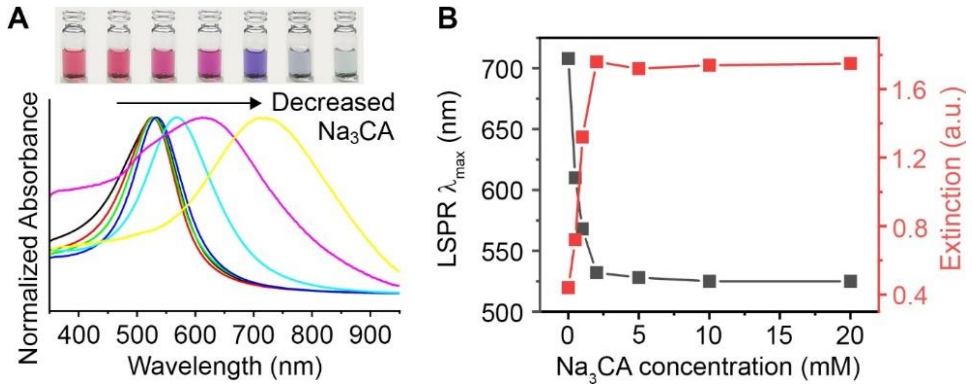

Figure S8. LSPR properties of hollow Au-Ag nanostructures obtained at varied concentrations of Na_3CA. (A) Photographs and corresponding extinction spectra of those nanostructures. Their TEM can be found in **Figure 2D** and **Figure S4B-G**. (B) A plot of the major LSPR peak (λ_{max}) in (A) against the concentration of Na_3CA in the growth.

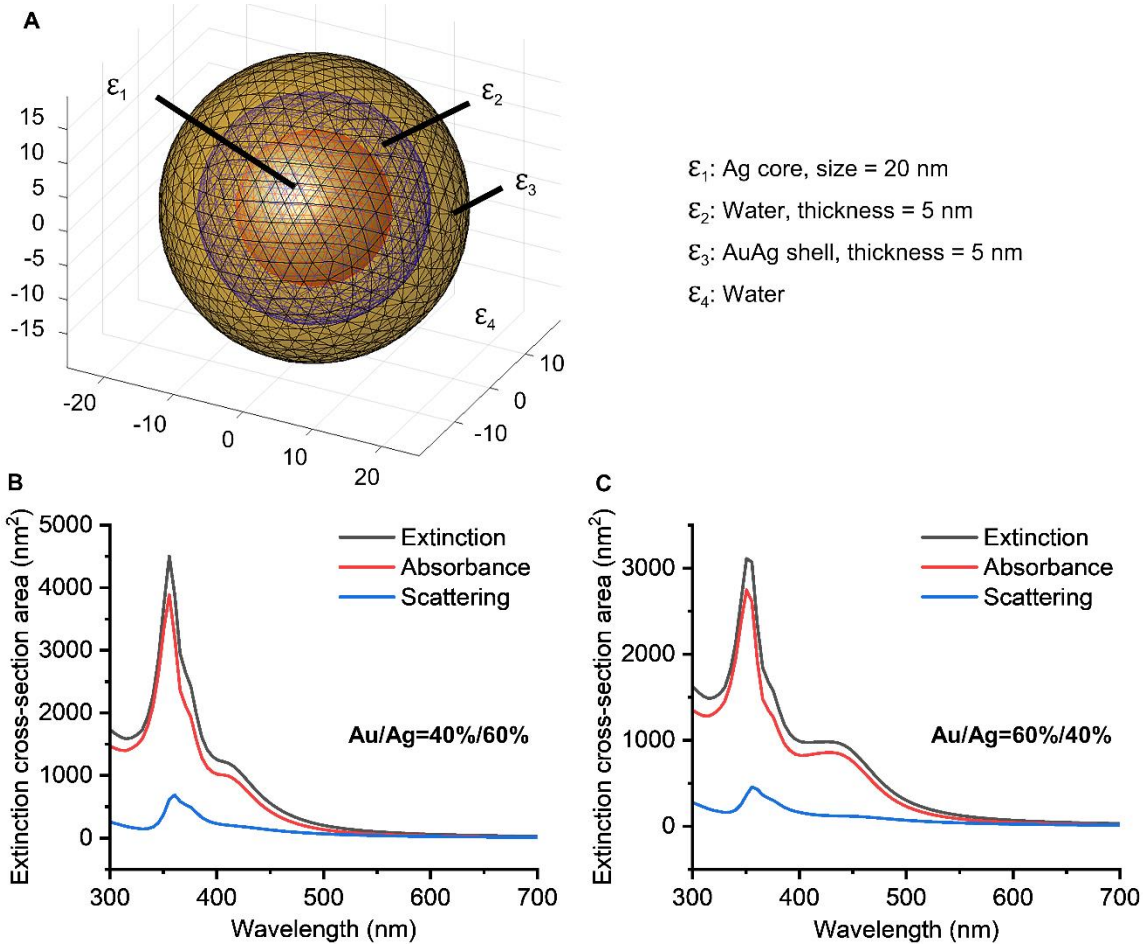

Figure S9. Simulation results of the extinction cross-section area of a sandwich Ag-water-AuAg core-void-shell structure with varied Au/Ag ratio in the shell. (A) The proposed model and corresponding parameters. (B, C) Simulation results of the extinction cross-section area for the model with Au/Ag molar ratio of 40%/60% (B) and 60%/40% (C) in the shell. All parameters ($\boldsymbol{\varepsilon}_{1\text{-}4}$) were kept unchanged.

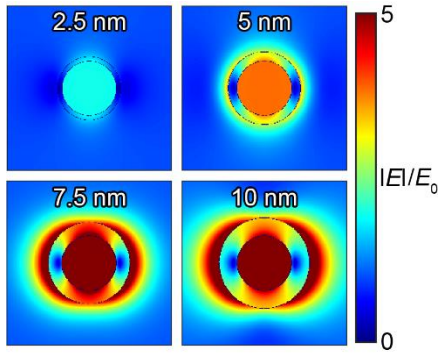

Figure S10. Electric field intensity maps (logarithmic scale) of the shells with varied thickness. The map was generated at the major LSPR extinction peak at 532 nm.

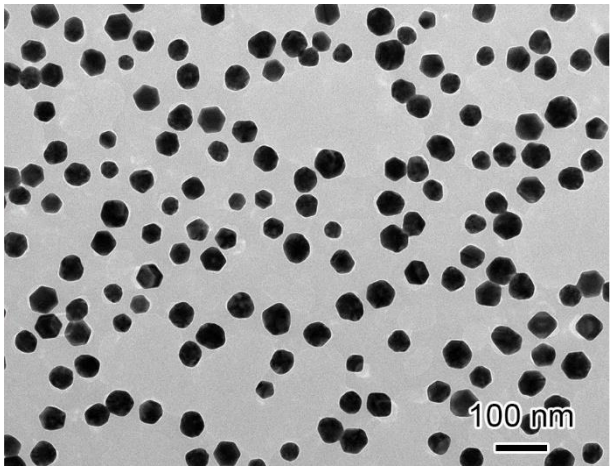

Figure S11. TEM image of 50 nm AuNPs.

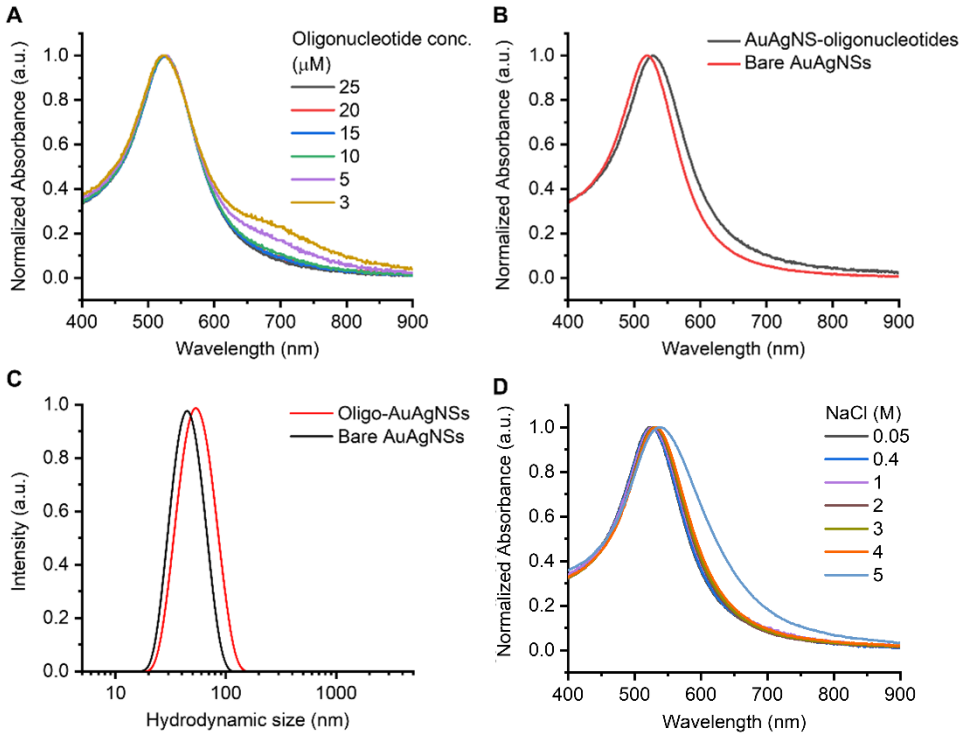

Figure S12. **Spectral monitoring and dynamic light scattering measurements of Au-Ag nanoshells (NSs) in conjugation with oligonucleotides.** (A) Titration of Au-Ag shells with oligonucleotides of different concentrations in the citrate-HCl buffer (50 mM, pH=3.0). The appearance of 700 nm peak suggests insufficient oligonucleotide coating that led to the NP aggregation. (B) Spectra of aqueous Au-Ag shells suspensions before and after mixing with 20 μM oligonucleotides. (C) Dynamic light scattering measurements of aqueous Au-Ag shells suspensions before and after mixing with 20 μM oligonucleotides. (D) The colloidal stability test by incubating the oligonucleotide-modified Au-Ag shells in sodium chloride (NaCl) solution with different concentrations. The barely changed spectra suggest good stability of oligonucleotide-modified Au-Ag shells against up to 4M NaCl. The sample tested in (B-D) were purified by multiple steps of washing to remove the free oligonucleotides.

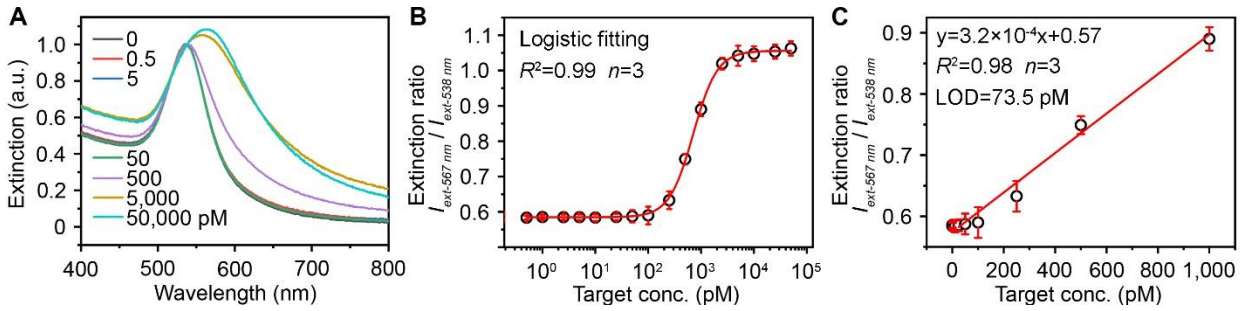

Figure S13. **Plasmonic coupling assay of oligonucleotides using using 50 nm AuNPs as sensors.** (A) Representative extinction spectra normalized at 538 nm taken from the assay solution with varied target concentrations. (B) Calibration curve generated by plotting the extinction ratio of $I_{ext\text{-}567\ nm}$ and $I_{ext\text{-}538\ nm}$ against target concentration. A logistic fitting is applied. (C) A linear range of the calibration curve shown in (C). Error bars indicate the standard deviations (n = 3).

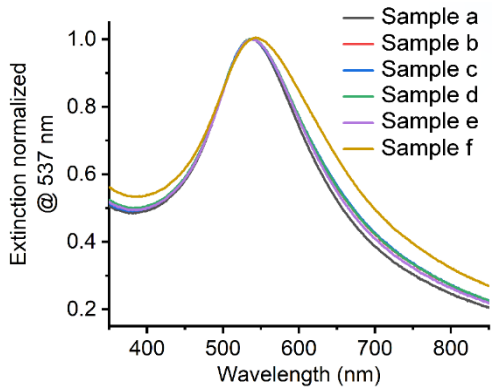

Figure S14. Plasmonic LAMP performance at varied conditions. Detailed conditions can be found in below Table.

Sample	Experimental conditions					Color change
	RT-LAMP	**Enzyme digestion**	**Heating denaturation**	**PCA**	**RNA input (cp/μL)**	
a	No	No	No	Yes	0	[a]No
b	Yes	No	No	Yes	0	No
c	Yes	No	No	Yes	10	No
d	Yes	Yes	No	Yes	10	No
e	Yes	No	Yes	Yes	10	No
f	Yes	Yes	Yes	Yes	10	Yes

[a]: This sample is used as a reference to indicate the color change.

Table S1. Sequence Information of the Target Oligonucleotide and Corresponding probes.

Name	Sequence (5'-3')
Target	CCCAGCGCTTCAGCGTTCTTCGGAATGTCGCGCATT
Probe A	[a]AAAAAAAAAAAAAAAAATGCGCGACATTCCGAA
Probe B	AAAAAAAAAAAAAAAGAACGCTGAAGCGCTGGG

[a]: The poly A tail included in the oligonucleotides is used to increase flexibility of the sequence. A thiol group is modified on the 5' side for both sequences.

Table S2. Sequence Information of the Primers, Enzyme Cutting Sites on the RT-LAMP Product, ssDNA as a Target for DNA Hybridization after the Heat Denaturation, and Probes shown in Figure 4A.

Name	Subtype	Sequence (5'-3')
Primers	F3	GCTGCTGAGGCTTCTAAG
	B3	GCGTCAATATGCTTATTCAGC
	FIP	GCGGCCAATGTTTGTAATCAGTAGACGTGGTCCAGAACAA
	BIP	TCAGCGTTCTTCGGAATGTCGCTGTGTAGGTCAACCACG
	FLP	CCTTGTCTGATTAGTTCCTGGT
	BLP	TGGCATGGAAGTCACACC
dsDNA		[a]CCGCAAATTGCACAATTTGCCCCCAGCGCTTCAGCGTTCTTCGGAATGTCGCGCATTGGCATGGA AGTCACACCTTCGGGAACGTGGTT
ssDNA		CAAATTGCACAATTTGCCCCCAGCGCTTCAGCGTTCTTCGGAATGTCGCGCATTGGCATGGAAGTC ACACCTTCGGGAACGTG
Probes	A	[b]AAAAAAAAAAAAAAACACGTTCCCGAAGGTGTGACT
	B	AAAAAAAAAAAAAAATCCATGCCAATGCGCGACATT
	C	AAAAAAAAAAAAAAACCGAAGAACGCTGAAGCGCTG
	D	AAAAAAAAAAAAAAGGGGCAAATTGTGCAATTTG

[a]: Red letters highlight the regions cut by enzymes. [b]: The poly A tail included in the oligonucleotides is used to increase flexibility of the sequence.